Applied Mathematics, Modeling and Computer Simulation
C.-H. Chen et al. (Eds.)

doi:10.3233/ATDE221027

Modeling of Autonomous Grasping Method for UAV Guided by Vision

Yunze ZHANG[a,1], Gaofeng YUE[b]

[a] *College of Information Engineering, Shenyang University, Shenyang 110044,China*
[b] *Schoole of Cyber Science and Engineering, Xi'an Jiaotong University, Xi'an 710049, China*

Abstract. For the current problems of separation of flight control and gripping control of the gripping UAV and redundancy of UAV degrees of freedom and robotic arm degrees of freedom. In this paper, the characteristics of multi-rotor UAV with high mobility and multiple degrees of freedom are used to replace the traditional mechanical gripper structure. At the same time, binocular vision technology is used for target information acquisition, the target position is converted into UAV flight attitude control commands, and conduct mathematical modeling and analysis of a multi-rotor grasping UAV.

Keywords. UAV, Autonomic grabbing, Visual guidance, Flight control

1. Introduction

With its advantages of high maneuverability and low cost, MUAV has made outstanding achievements in aerial photography, intelligent logistics, fixed-point delivery and disaster relief support[1]. A large number of functional UAV have emerged, but these products only use UAVs as carriers, which cannot reflect the integration and intelligence of their products. With the rapid development of machine vision technology, UAVs' autonomous decision-making by virtue of visual information has been hotly studied by scholars.

There is deep research on grasping UAV abroad. At present, many researchers carry grippers on UAV platforms, usually using joints with more than six degrees of freedom. [2] Due to the influence of load in the grasping process, the dynamic performance of UAV decreases[3]. The unmanned flying robot equipped with a 7-degree-of-freedom industrial robot arm developed by the German Aerospace Center in 2013 can grasp objects placed vertically on the ground. Through the dynamic decoupling of the aircraft and the robot arm, the divergent oscillation of the aircraft and the robot arm is reduced, and the grasping success rate is improved[4]. In 2014, Danko et al. proposed a grasping drone equipped with a 3-degree-of-freedom mechanical fixture[5], which greatly reduced the degree of freedom of the mechanical arm and increased the load capacity. Unfortunately, there is still some redundancy in the degree

[1] Corresponding Author, Yunze ZHANG, College of Information Engineering, Shenyang University, Shenyang 110044,China; E-mail: zhyz96@163.com

of freedom; Zain Anwar Ali et al. proposed the UAV grasping system based on 8 degrees of freedom in 2019[6], The UAV acts as six degrees of freedom, and the gripper has two degrees of freedom. The adaptive controller is used to optimize the uncertain interference of the aircraft, and the stability of the control system is proved by Lyapunov equation, which has made a breakthrough in grasping the UAV system.

However, there is little research on grasping UAV in China, Song Dalei, Meng Xiangdong and others put forward the dynamic modeling method of 3-DOF rotor flight manipulator in 2015[7], which eliminated the error of the end effector by compensating the disturbance caused by the hovering of the UAV, and realized the principal feasibility of the model by simulation. However, computer vision technology was not incorporated into the UAV and lacked autonomy; In 2017, Du Yegui et al. proposed the grasping control system of flight manipulator based on visual servo[8], The MR-UAV is equipped with a rotatable camera and a lightweight manipulator, and the UAV-multi-degree-of-freedom manipulator composite model is established in three-dimensional space. The image acquisition system is designed and the spatial capture task is completed by hand-eye system, but the collected images are not fused.

2. UAV Stereo Vision

On the premise of allowing camera lens distortion error, the traditional camera conforms to the pinhole imaging model. As shown in the figure 1, a certain point $P=[x,y,z]^T$ in three-dimensional space and its image Q $p=[u,v]^T$ on the image plane meet the following requirements:

$$\begin{cases} u=(x\cdot b)/z \\ v=(y\cdot b)/z \end{cases} \tag{1}$$

Where, b is the focal length of the camera.

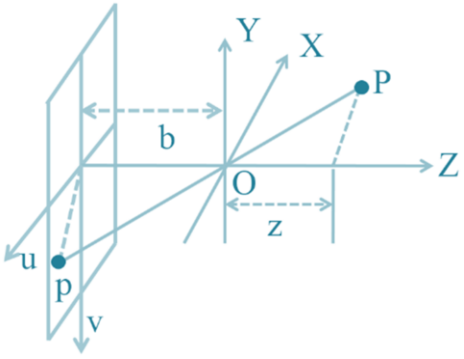

Figure 1. Pinhole model.

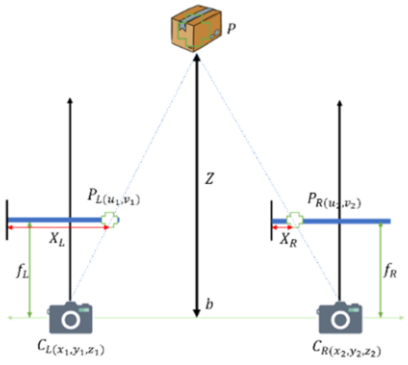

Figure 2. Basic principles of binocular vision.

Because of the loss of depth information in perspective imaging process, it is generally impossible to directly infer the actual three-dimensional coordinates of object points from image points. Binocular vision cameras just make up for this deficiency.

Binocular vision system obtains multiple images from different angles by a single camera or digital images of observed objects by two cameras at the same time[9-11]. Its core is the modeling of geometric parallax principle, and its basic principle is shown in figure 2.

Where f_L and f_R are the focal lengths of left and right cameras, B is the baseline distance, the position of a certain point $P(X,Y)$ of the object in the images collected by left and right cameras is $P_L(u_1,v_1)$, $P_R(u_2,u_2)$, $C_L(x_1,y_1,z_1)$ and $C_R(x_2,y_2,z_2)$ are the mapping points of image P_L and P_R in the projection plane.

Assuming that the left and right image acquisition planes are in the same plane, that is, $v_1 = v_2$ in points $P_L(u_1,v_1)$ and $P_R(u_2,v_2)$, there is a triangular geometric relationship to obtain equation (2).

$$\begin{cases} f_L = f_R = f \\ u_1 = f\dfrac{x_1}{z_1}, u_2 = \dfrac{x_1 - b}{z_1} \\ v_1 = v_2 = f\dfrac{y_1}{z_1} \end{cases} \tag{2}$$

Equation (3) is obtained by comparing the position difference of point P in two images.

$$d = (u_1 - u_2) = f\frac{b}{z_1} \tag{3}$$

Through the above analysis, as long as the corresponding points of a certain point in space on the left and right image planes are determined, and the internal and external parameters of the camera are obtained by camera calibration, the spatial three-dimensional coordinates of a certain point P in space can be calculated, as shown in Equation (4).

$$x_1 = b\frac{u_1}{d}, y_1 = b\frac{v_1}{d}, z_1 = b\frac{f}{d} \tag{4}$$

For the convenience of research, assuming that the centroid coordinates of the captured target coincide with the origin of the world coordinate system, any point $[X\ Y\ Z\ 1]^T$ in the captured target is mapped to the image plane $[x\ y\ 1]^T$, as shown in equation (5).

$$\lambda\begin{bmatrix} x \\ y \\ 1 \end{bmatrix} = \begin{bmatrix} f_x & 0 & c_x \\ 0 & f_y & c_y \\ 0 & 0 & 1 \end{bmatrix} P_0 T^{-1} \begin{bmatrix} X \\ Y \\ Z \\ 1 \end{bmatrix} \tag{5}$$

Where $P_0 = \begin{bmatrix} I_{3\times3} & 0_{3\times1} \end{bmatrix}$ and T are homogeneous transformation matrices between world coordinate system and camera coordinate system, f_x and f_y are focal length lengths in x and y directions, c_x and c_y are focal length pixels in x and y directions, and λ is an arbitrary scale transformation factor. It is impossible for the aircraft to keep flying in the same horizontal plane in space all the time, and the motion attitude of the UAV will inevitably lead to the tilt of the camera and the slant of the image imaging plane, in other words, it will affect the position coordinates of the target in the image plane. The relationship between the target coordinates and the UAV attitude is shown in figure 3.

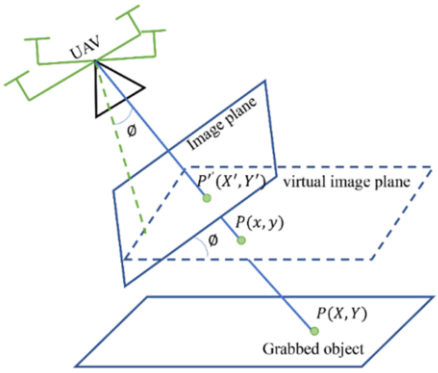

Figure 3. Sketch of image plane transformation under attitude.

Set the virtual image plane, which is always parallel to the object placement plane, and its area size is 1280×1080, and carry out matrix transformation on a certain point P in the space of the two image planes, as shown in Equation (6),

$$\begin{bmatrix} x \\ y \\ 1 \end{bmatrix} = \begin{bmatrix} \cos\phi & -\sin\phi & t_x \\ \sin\phi & \cos\phi & t_y \\ 0 & 0 & 1 \end{bmatrix} \begin{bmatrix} X' \\ Y' \\ 1 \end{bmatrix} \tag{6}$$

Where ϕ is the first Eulerian angle change of UAV in space, t_x and t_y are the translations of point P in x and y directions. Through the above derivation, the position information of any point in the captured object in the centre virtual image plane (i.e. flight plane) with unit focal length is obtained, that is, the transformation from F_w coordinate system to F_c coordinate system.

3. UAV Flight Control

The control methods of MR-UAV are all based on aircraft dynamics model, and Four-Rotor unmanned aerial vehicle (FR-UAV) is a common type of MR-UAV[12-14]. Figure 4 shows the coordinate system and related parameters of a quad-rotor aircraft. F_w is positioned as a global coordinate system, usually using NED (North (N)-East (E)-Down (D)) coordinate system, and the coordinate system fixed with the aircraft is F_b. Assuming that the geometric centres and centroids of F_b and FR-UAV coincide, the X_b direction of F_b is defined as the front of FR-UAV, and the Y_b direction is the right side of FR-UAV, while Z_b can be obtained by right-hand coordinate system rule.

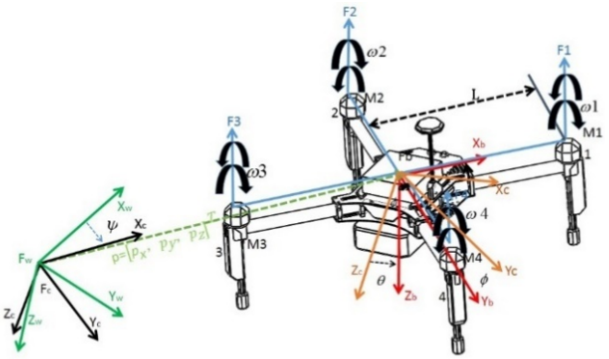

Figure 4. FR-UAV relevant coordinate system and parameters.

Assuming that the spatial position relationship of aircraft in F_w coordinate system is not considered. Assuming that F_w and F_b coincide, F_b first rotates around Z_w axis in F_w coordinate system to obtain yaw angle (yaw), then defines it as coordinate system Y_c, then rotates around Y_c axis to form pitch angle (pitch) to obtain new coordinate system F_d, and finally F_d rotates around X_d axis to form roll angle (roll). After the transformation of the above three coordinate systems, the final aircraft attitude can be obtained. Assuming that the distance from the motor to the center of mass of the aircraft in figure 4 is L, the following aircraft dynamic equations can be obtained by physical derivation[15-17].

$$\begin{cases} \dot{v} = g e_3 + \dfrac{1}{m} R\ f_z\ e_3 \\ \dot{R} = R\ \Omega \\ \dot{\omega} = J^{-1}\ \tau - J^{-1}\ \Omega\ \omega_b \\ \dot{p} = [v_x, v_y, v_z]^T \end{cases} \tag{7}$$

Where $\dot{v}$ is the velocity of UAV in the x, y and z axes in the global coordinate system F_w, g is the acceleration of gravity, m is the mass of UAV, f_z is the total

lift generated by the UAV motor, $e_3 = \lceil 0,0,1 \rceil^T$, The direction of $f_z e_3$ is opposite to the Z_b axis under F_b, R is the rotation matrix of F_b relative to F_w, $\omega_b = [\omega_X, \omega_Y, \omega_Z]^T$ is the triaxial angular velocity of FR-UAV relative to the global coordinate system, which is also its own variable in the FR-UAV airframe coordinate system F_b, Ω is the matrix expression of ω_b, τ is the torque moment generated by the aircraft relative to its own center of mass, J is the moment of inertia of the aircraft, and p is the position of the aircraft in the global coordinate system F_w. The calculations of Ω, τ and p are shown in equations (8), (9) and (10).

$$\Omega = \omega_b^{\wedge} = \begin{bmatrix} 0 & -\omega_z & \omega_y \\ \omega_z & 0 & -\omega_x \\ -\omega_y & \omega_x & 0 \end{bmatrix} \tag{8}$$

$$\tau = \begin{bmatrix} \tau_x & \tau_y & \tau_z \end{bmatrix}^T \tag{9}$$

$$p = \begin{bmatrix} p_x & p_y & p_z \end{bmatrix}^T \tag{10}$$

From the equations of states (7)-(10), it can be seen that FR-UAV has 12 states: velocity $v = \begin{bmatrix} v_x & v_y & v_z \end{bmatrix}^T$, attitude R (expressed as three Euler angles), position $p = \begin{bmatrix} p_x & p_y & p_z \end{bmatrix}^T$, At the same time, the system also has four inputs, namely f_z and $\tau = \begin{bmatrix} \tau_x, \tau_y, \tau_z \end{bmatrix}^T$. Assuming that the rotational angular velocity of each motor is ω_i, the thrust and counter torque are shown in Equation (11).

$$\begin{cases} F_i = k_F \omega_i^2 \\ M_i = k_M \omega_i^2 \end{cases} \tag{11}$$

Where k_F and k_M are constant coefficients, the relationship between input and output can be obtained by equation (7), such as equations (12) and (13).

$$\begin{cases} f_z = F_1 + F_2 + F_3 + F_4 \\ t_X = (F_2 - F_4) \times L \\ t_Y = (F_1 - F_3) \times L \\ t_Z = -M_1 + M_2 - M_3 + M_4 \end{cases} \tag{12}$$

$$\begin{bmatrix} f_z \\ \tau_X \\ \tau_Y \\ \tau_Z \end{bmatrix} = \begin{bmatrix} k_F & k_F & k_F & k_F \\ 0 & k_F L & 0 & -k_F L \\ k_F L & 0 & -k_F L & 0 \\ k_M & k_M & k_M & k_M \end{bmatrix} \begin{bmatrix} \omega_1^2 \\ \omega_2^2 \\ \omega_3^2 \\ \omega_4^2 \end{bmatrix} \tag{13}$$

Through the above derivation, the dynamic model of FR-UAV can be obtained, and various motions of FR-UAV in space can be realized by controlling the four ω or four motor speeds in equation (13).

4. Conclusion

The purpose of this paper is to make an in-depth study on grasping UAV. By introducing binocular vision technology, using the characteristics of strong maneuverability and multi-degree of freedom of multi-rotor UAV instead of the multi-degree of freedom of traditional mechanical gripper, the multi-rotor grasping UAV is re-modeled and analyzed, and the autonomous grasping method of multi-rotor UAV based on binocular vision is modeled. The follow-up research will further focus on the actual test.

References

[1] Zhang Xin. Research on attitude and navigation information fusion algorithm of multi rotor UAV [D]. Graduate School of Chinese Academy of Sciences (Changchun Institute of optics, precision machinery and Physics), 2015.
[2] KIM S, CHOI S and KIM HJ. Aerial manipulation using a quadrotor with a two DOF robotic arm[C].In: Proceedings of the IEEE/RSJ international conference on intelligent robots and systems, Tokyo, Japan 2013, 4990–4995.
[3] PANNIR MPO, APARNA MN and JENCY MVP. Design and development of an autonomous UAV using image processing algorithm for precision agriculture[J]. IJAICT 2018, 4: 1358–1360.
[4] HUBER F, KONDAK K, KRIEGER K, et al. First analysis and experiments in aerial manipulation using fully actuated redundant robot arm[C]//IEEE/RSJ International Conference on Intelligent Robots and Systems. Piscataway, USA: IEEE, 2013: 3452-3457.
[5] DANKO T W and OH P Y. Design and control of a hyper redundant manipulator for mobile manipulating unmanned aerial vehicles[J]. Intell Robot Syst 2014;73(4): 709–723.
[6] ZAIN A A and XINDE L. Modeling and controlling of quadrotor aerial vehicle equipped with a gripper[J]. Measurement and control,2019,5,1:6.
[7] SONG D L, MENG X D, QI J T and HAN J D. Dynamics Modeling and Predictive Control Method for 3-DOF Rotor Flying Manipulator System [J]. Robot, 2015,37(02): 152-160.
[8] DU Y G. Grasping control of flight manipulator based on visual servo [D]. Harbin University of Technology, 2017.
[9] NARAYAN M, BAISAKHI C, DEBASHIS N. Relative velocity measurement using low-cost single camera-based stereo vision system[J]. Measurement, 2019, 141:1-11.
[10] TAYLOR Z, NIETO J. Motion-Based Calibration of Multimodal Sensor Extrinsic and Timing Offset Estimation [J]. IEEE Transactions on Robotics, 2016, 32(5):1215–1229.
[11] MARCIN C, MICHAL M, MIROSLAW N, GRZE-GORZ K. The mathematical model of UAV vertical take-off and landing[J]. Aircraft Engineering and Aerospace Technology, 2019, 91(2):249-256.
[12] Navdeep, SONAL G, ASHA R, VIJANDER S. An improved local binary pattern based edge detection algorithm for noisy images[J]. Journal of Intelligent& Fuzzy Systems, 2019, 36(3):2043-2054.
[13] Chen Xiaoqiao, Ye Xiaohan,Hu Ting, Xia Tong. Positioning and control system of UAV based on binocular vision[J]. Journal of Wuhan University (Engineering Edition),2017,50(04):624-629.
[14] Huang X.X., Yan J.G., Zhang Y.K. Hardware design of small UAV navigation system[J]. Science, Technology and Engineering,2012,12(23):5832-5836.
[15] Wang Zhengyu, Xian Bin. Finite-time convergence control design of a tilting tri-rotor UAV[J]. Control Theory and Applications,2019,36(09):1442-1452.
[16] Han Xiaowei, Yue Gaofeng. Quadrotor UAV gyro array data fusion algorithm[J]. Journal of Instrumentation,2019,40(08):213-221.
[17] Wang J, Zhang YH, Li XP. Simulation of attitude control method for combined UAV navigation system[J]. Computer Simulation,2019,36(06):73-76+82.